VIP *Very Important Paper*

Special Collection

Consensus Virtual Screening Identified [1,2,4]Triazolo[1,5-*b*] isoquinolines As MELK Inhibitor Chemotypes

Anita Rácz,[a, b] Roberta Palkó,[b, c] Dorottya Csányi,[b] Zsuzsanna Riedl,[b] Dávid Bajusz,*[b] and György M. Keserű[b]

Maternal Embryonic Leucine-zipper Kinase (MELK) is a current oncotarget involved in a diverse range of human cancers, with the usage of MELK inhibitors being explored clinically. Here, we aimed to discover new MELK inhibitor chemotypes from our in-house compound library with a consensus-based virtual screening workflow, employing three screening concepts. After careful retrospective validation, prospective screening and *in vitro* enzyme inhibition testing revealed a series of [1,2,4]triazolo[1,5-*b*]isoquinolines as a new structural class of MELK inhibitors, with the lead compound of the series exhibiting a sub-micromolar inhibitory activity. The structure-activity relationship of the series was explored by testing further analogs based on a structure-guided selection process. Importantly, the present work marks the first disclosure of the synthesis and bioactivity of this class of compounds.

Introduction

Maternal Embryonic Leucine-zipper Kinase (MELK) is a member of the AMPK/Snf1 kinase family and involved in mammalian embryonic development. Although its serine/threonine kinase domain is highly conserved in mammalian and non-mammalian species as well,[1] the function of MELK is slightly different in each species. MELK has diverse functions in cellular processes and plays important roles in cell cycle regularization, proliferation and oncogenesis.[2] Additionally, the overexpression of MELK is observed in many human cancers (tumor initiation and propagation processes) such as lung cancer,[3] colon tumor,[4] rectal cancer,[5] prostate cancer[6] or melanoma.[7,8]

Since MELK is reported as a promising oncotarget, several drug discovery efforts have been made to find potential MELK inhibitors. Chung and colleagues performed a high throughput screen and optimized the hits with structure-based drug design focused to the active site of the kinase. They identified a highly potent inhibitor OTSSP167 (alternatively called OTS167), with an IC_{50} of 0.41 nM.[9] The compound additionally inhibits multiple mitotic kinases[10] and can be effective against pediatric brain tumor[11] and acute myeloid leukemia.[12] Beke et al. reported another potent and cell permeable MELK inhibitor MELK-T1 (with an IC_{50} of 0.37 nM), which can additionally trigger the proteasome-mediated degradation of MELK.[13] As MELK is highly expressed in triple negative breast cancer (TNBC), Edupuganti and coworkers have identified 5-substituted indolinones with subnanomolar K_i in a targeted screen, which can inhibit Mcl-1 expression in a MELK-expressing TNBC cell line.[14,15] Juane and coworkers found that the biguanide-derived compound CRO15 targets both MELK and AMPK, which can be an effective way for novel melanoma therapies.[16] Wang et al. designed and synthesized 1H-pyrrolo[2,3-*b*]pyridine derivatives as potential inhibitors of MELK and they have found a compound with an IC_{50} of 32 nM against MELK.[17] While earlier virtual screening efforts relied on homology modeling,[18] currently 31 crystal structures of MELK (homo sapiens) are available in the PDB database[19,20] for structure-based virtual screening efforts toward new inhibitors.

Complementing our earlier works where MELK inhibition was investigated in the broader context of introducing a new kinase hinge binder scaffold,[21] or new covalent warheads,[22] here we have developed a complex, structure- and ligand-based drug design protocol specifically to find new MELK inhibitors. Following enzyme-based *in vitro* validation, an additional optimization step based on the structure–activity relationship (SAR) of the discovered [1,2,4]triazolo[1,5-*b*] isoquinoline series yielded a sub-micromolar MELK inhibitor with this new core scaffold.

[a] *Dr. A. Rácz*
Plasma Chemistry Research Group
Research Centre for Natural Sciences
Magyar tudósok krt. 2, 1117 Budapest (Hungary)
[b] *Dr. A. Rácz, Dr. R. Palkó, D. Csányi, Prof. Z. Riedl, Dr. D. Bajusz, Prof. G. M. Keserű*
Medicinal Chemistry Research Group
Research Centre for Natural Sciences
Magyar tudósok krt. 2, 1117 Budapest (Hungary)
E-mail: bajusz.david@ttk.hu
[c] *Dr. R. Palkó*
Present affiliation: Organocatalysis Research Group
Research Centre for Natural Sciences
Magyar tudósok krt. 2, 1117 Budapest (Hungary)

Supporting information for this article is available on the WWW under https://doi.org/10.1002/cmdc.202100569

Special Collection *This article belongs to the Early-Career Special Collection, "EuroMedChem Talents".*

Results and Discussion

To discover new MELK inhibitors, we have assembled a consensus-based virtual screening workflow, employing three orthogonal computational methods: ligand docking, pharmacophore screening and shape screening. Prior to applying the workflow for prospective purposes, each of the screening methods were thoroughly validated retrospectively, on a dataset of 50 known, potent MELK inhibitors (< 100 nM IC_{50}) extracted from the ChEMBL database,[23,24] and 2544 decoy molecules.[25] For ligand docking, seven PDB structures were selected based on the diversity of their binding site conformations, and the geometric mean of the Glide SP docking scores was used as the data fusion rule for ensemble docking.[26] For pharmacophore screening, a consensus model was developed based on 40 known actives and 10 known inactives. For shape screening, the most active inhibitor with an experimentally determined binding mode was used as the query. The workflow is summarized in Figure 1, and retrospective performances of the models are reported in the Experimental section.

After retrospective validation, the models were used prospectively in a consensus effort to discover new MELK inhibitors from our in-house database of 2208 compounds. The in-house database contains molecules that were synthesized for diverse projects, corresponding to 941 unique Murcko scaffolds,[27] 82 of which are represented by five or more compounds. The majority of the compounds was not yet tested for kinase inhibition, apart from a series of indazoles we recently reported as JAK2 inhibitors.[28] In the prospective screening, a molecule was selected for *in vitro* testing if it was predicted to be active by at least two of the three models (docking, shape and pharmacophore). Ultimately, 64 compounds were selected and evaluated for their inhibitory activities against MELK in a FRET-based biochemical assay. (Results of the initial, single-point screen are reported in Table S1 and Figure S1.)

Dávid Bajusz received his PhD in chemistry from the Budapest University of Technology and Economics. Since 2017, he has been employed as a postdoctoral researcher in the Medicinal Chemistry Research Group, led by György M. Keserű, at the Research Centre for Natural Sciences in Budapest, Hungary. His main research interests include medicinal chemistry, computational drug discovery and cheminformatics. He is involved in several international collaborative research efforts in these areas, focusing on drug discovery for pharmaceutical targets of oncological indications, as well as methodological innovations in computational drug design. He has co-authored more than 40 publications, as well as three book chapters in major reference works, and was awarded for his accomplishments with the Junior Prima Prize in the category of Hungarian Science in 2019. In addition to his research work, he has co-organized several conferences and regularly provides peer reviews for major scientific journals of his field. Since 2020, he is a recipient of the János Bolyai Research Scholarship of the Hungarian Academy of Sciences.

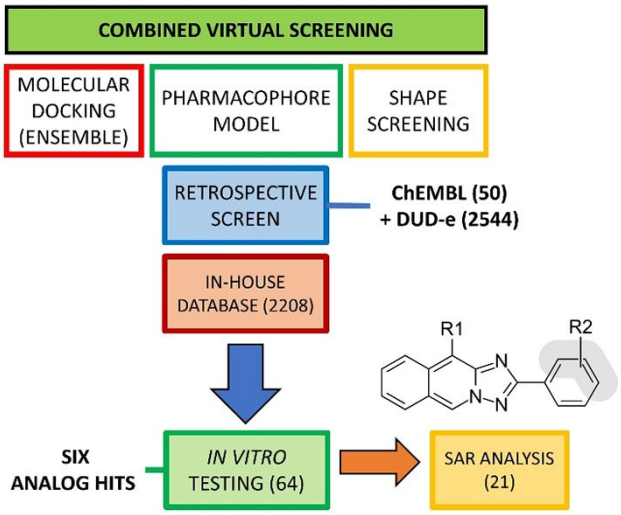

Figure 1. Workflow of the computational screening and experimental testing steps, with the respective compound counts. Three virtual screening concepts (docking, pharmacophore and shape screening) were used in parallel. These were validated retrospectively and applied prospectively to our in-house compound database. Compounds that are predicted as actives by at least two out of three screening concepts were considered as virtual hits and selected for primary *in vitro* testing, followed by an SAR analysis of the [1,2,4]triazolo[1,5-*b*]isoquinoline scaffold.

The primary, single-point screen revealed nine compounds with percent inhibition values over 40% at 10 μM concentration and interestingly, six of these (**1**, **2**, **4**, **5**, **8**, **19**) belonged to the same core scaffold: 2-phenyl-[1,2,4]triazolo[1,5-*b*]isoquinoline. (One further primary hit was the closely related 2-phenyl-[1,2,4]triazolo[3,2-a]isoquinoline – ID 1855.[29]) A quick search in the ChEMBL database reveals that this core scaffold was reported neither for MELK inhibition, nor any other biochemical activity earlier, marking our result as the first reported bioactivity of this scaffold. Also, apart from two prototypic compounds **1** and **2**,[30] no general synthesis was published for this chemotype.

Encouraged by these observations, we sought to understand the structure–activity relationship of this series. Therefore, we proceeded by evaluating the enzymatic IC_{50} values of the six confirmed hit compounds. These are summarized in Table 1, along with the percent inhibition values of seven more primary virtual hits with the same scaffold: compounds **3**, **6**, **7**, **13**, **14**, **20** and **21** (here, compound **13** was the only one where the IC_{50} value could be quantified).

The early SAR of this series immediately highlights two requirements for inhibitory activity: (i) a small apolar substituent in the 10 position of the [1,2,4]triazolo[1,5-*b*]isoquinoline core, and (ii) a methyl or methoxy substituent on the 2-phenyl unit.

Furthermore, the results hint at a preference for an ethyl (instead of methyl) group in the 10 position, as seen from the 2.5-fold activity boost of compound **19** in comparison to compound **5**.

Table 1. Structure–activity relationship of the [1,2,4]triazolo[1,5-*b*] isoquinoline-based MELK inhibitors.

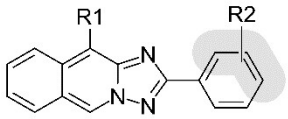

#	R1	N[a]	R2	IC_{50} [μM][b]
1[c]	Me			25.2
2[c]	Et		4-Me	4.82
3	Me		3-Cl	16% @ 10 μM
4	Me		4-OMe	3.67
5	Me		3-OMe	4.93
6	Me		3,4-Me-dioxy	39% @ 10 μM
7	Me		3-CF_3	20% @ 10 μM
8	Me		4-CF_3	45% @ 10 μM
9	Me	3		27% @ 10 μM
10	Me	3	4-Cl	13% @ 10 μM
11	Me	2		6.30
12	Me	4		30% @ 10 μM
13	Me		2,4-diCl	24.1
14	Me		3,4-diCl	18% @ 10 μM
15	Et		2-Cl	25% @ 10 μM
16	Et		3-Cl	18% @ 10 μM
17	Et		4-Cl	>3.7
18	Et		4-OMe	0.794
19	Et		3-OMe	2.04
20			3-Cl	15% @ 10 μM
21			3-Me	33% @ 10 μM

[a] Position of the nitrogen heteroatom in the terminal (rightmost) ring (gray area). [b] For compounds with low activity, percent inhibition values are reported at 10 μM concentration. [c] Syntheses for these compounds were reported earlier.[30]

To further evaluate the possible role of the ethyl group in position 10 and to explore other substitutions of the 2-phenyl unit, we have carried out a substructure search of our compound database, which revealed 21 additional compounds with the same core scaffold. From these, we have selected eight further compounds for *in vitro* testing, with a structure-guided approach, based on their predicted binding poses in the active site of MELK, overlaid on 14 PDB structures containing sub-micromolar MELK inhibitors with experimentally determined binding modes (Figure 2). Interestingly, many of the co-crystallized MELK inhibitors, as well as our inhibitor series, exhibit binding modes with only one hydrogen bond acceptor acting as an anchoring group toward the hinge region, instead of the 3-point donor-acceptor-donor motif that is typical for other kinases.[33]

The eight follow-up compounds represent two subclasses: (i) compounds **9**–12 contain pyridyl rings in place of the 2-phenyl unit, enabling us to explore the effect of an H-bond accepting heteroatom in either position of this ring, while (ii) compounds **15**–**18** contain an ethyl group in position 10, with chloro substituents in varying positions of the 2-phenyl unit (**15**–**17**), or a methoxy group in the 4 position (**18**).

From the first series, only compound **12** exhibited a significant inhibitory activity, suggesting that a heteroatom can only contribute to the binding affinity from position 2 of the 2-phenyl unit (Figure 2B). This contrasts with the increased affinity of methoxy analogues in positions 3 (**5**) or 4 (**4**), suggesting that the methoxy group does not act as a hinge-binding moiety (Figure 2A).

As for the 10-ethyl series, the chloro scan reveals a preference for the 4 position of the 2-phenyl unit as the ideal point of substitution, with compound **17** being the only chloro-substituted analogue with a significant (single-digit micromolar) inhibitory activity. Additionally, the 10-ethyl-2-(4-methoxyphenyl) analogue (**18**) is highlighted as the lead compound of this series with a sub-micromolar activity, presenting 2.5- and 4.5-fold activity boosts over its 3-methoxyphenyl (**19**) and 10-methyl (**4**) counterparts, respectively. These observations, along

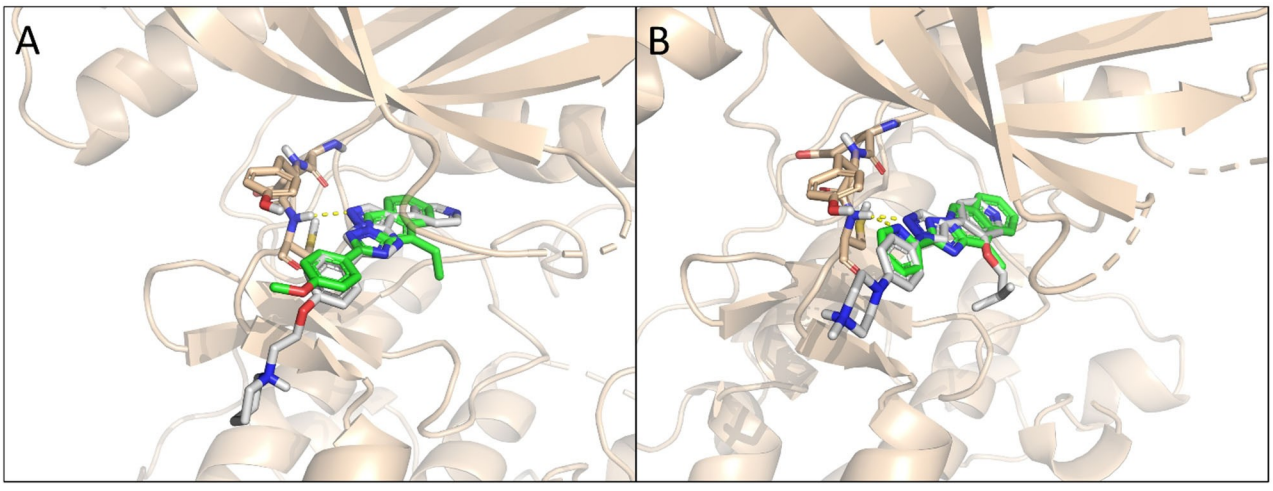

Figure 2. Structure-guided selection of further analogues for testing. A) Predicted binding mode of compound **18** (green sticks) overlaid on the binding mode of dorsomorphin (white sticks, PDB: 6GVX[31]). In addition to the good overlay of the respective cores, the 4-OMe group of **18** mimics the larger, solvent-exposed substituent of dorsomorphin, while the 10-ethyl group extends inside the binding pocket. B) Predicted binding mode of compound **11** (green sticks) overlaid on the binding mode of the MELK inhibitor NVS-MELK8F (white sticks, PDB: 5IHA[32]). Here, the heterocyclic nitrogen of the pyridyl unit can act as the anchoring group against the backbone NH group of the hinge residue C89, while the advantageous position of the 10-methyl group is supported by the hydrophobic group of NVS-MELK8F in the same position.

with the binding mode comparisons in Figure 2 provide ample support for positions 10 (main core) and 4 (2-phenyl unit) as the main drivers of the SAR and potential growing vectors of this MELK inhibitor series.

Comparison of the compound pairs **2** and **18** (4-methyl vs. 4-methoxy), as well as **4** and **18** (10-methyl vs. 10-ethyl) shows activity boosts within one order of magnitude. We observed similar trends between **1** (10-methyl, 4-unsubstituted) and **18**, or **8** (10-methyl, 4-trifluoromethyl) and **18**, revealing that the combination of these changes improves the activity by almost two orders of magnitude.

Finally, we note that this work marks the first general synthesis of the [1,2,4]triazolo[1,5-*b*]isoquinoline chemotype (see compounds **3**–**21**) *via* the reaction of the appropriate 2,3-diamino-isoquinolinium 4-methylbenzenesulfonates and aryl aldehydes, as detailed in the Experimental section.

Conclusion

MELK is a current and important oncotarget, involved in multiple types of human cancer. While there are a few compounds in clinical development, an approved MELK inhibitor drug is still missing, highlighting the importance of exploring the chemical space to identify new inhibitors with diverse structural features. Here, we aimed to explore our in-house compound collection by means of a consensus-based virtual screening methodology, employing three orthogonal screening concepts (docking, shape and pharmacophore screening). After thorough retrospective validation on known MELK inhibitors, the workflow was applied prospectively to screen a database of 2208 compounds, which ultimately resulted in the discovery of 2-phenyl-[1,2,4]triazolo[1,5-*b*]isoquinoline as a new MELK inhibitor chemotype, including the 10-ethyl-2-(4-methoxyphenyl) analogue **18** with a sub-micromolar inhibitory activity. Apart from two prototypic compounds, this is the first disclosure of their general synthesis. Importantly, our findings have not only widened the chemical space of known MELK inhibitors, but also provided the first reported bioactivity for the 2-phenyl-[1,2,4]triazolo[1,5-*b*]isoquinoline core.

Experimental Section

Computational methods

Ligand set preparation. A retrospective ligand set was created for evaluating our virtual screening protocol. Active MELK inhibitors (annotated with the UniProt[34,35] ID of MELK) with IC_{50} values below 100 nM were selected from the ChEMBL database.[23,24] In the next step, the RDKit[36] Diversity picker node was used in KNIME[37] (version 4.3.2) for the selection of fifty diverse compounds based on their fingerprints and the calculated Tanimoto distances. The decoy set was generated online with DUD-E (Database of Useful Decoys – Enhanced).[25] In total, 2594 different molecules were used as a retrospective set including 50 actives (ChEMBL IDs are included in Table S3) and 2544 inactives. Schrödinger (version 2020–4) LigPrep module was used to generate 3D structures of the molecules with the dominant protonation state.[38] After the ligand preparation the dataset contained 4996 entries (with tautomers and stereoisomers). The in-house database containing 2208 molecules was prepared in the same way and was used as a prospective screening set.

Ligand docking. Twenty-three X-ray crystal structures of MELK with resolutions below 3 Å were downloaded from the PDB database.[19,20] Hierarchical clustering of the binding site residues with max. 5 Å distance from the ligands was performed with Scipy[39] (version 1.5.2) based on the Euclidean distance with complete linkage. Seven representative structures (4BKZ,[40] 4D2T, 4D2 W, 4UMP,[41] 5MAH,[42] 5TWZ, 5TX3[43]) were selected for further application in docking as the centroids of each cluster defined at a distance threshold of 0.5 Å (the dendrogram is reported in Figure S2). Schrödinger Glide (with the SP scoring function) was applied for ensemble docking,[44,45] and geometric mean, minimum and maximum values of the seven docking scores were calculated for the final ranking of the ligands.[26] AUC values of the ROC curves were calculated for the retrospective study.[46] Figure 3 shows the result of the retrospective docking in the case of four different protein structures as examples and the three data fusion methods. From these, the geometric mean was chosen based on its AUC value of 0.93 and our earlier results on data fusion rules,[26] Glide docking scores were multiplied by −1 to allow for the calculation of geometric means. Compounds were classified as active above a fused Glide docking score of 6.09 (based on the minimum Euclidean distance from the [0;1] point, which represents ideal classification in the ROC plot with an AUC value of 1).

Shape screening. Shape screening was also performed in the Schrödinger platform,[48] with the use of the 5IHC crystal structure, which contains the most active ligand in the binding site (IC_{50} of 13 nM).[32] Three types of volume scoring were tested in the screen: typed pharmacophore, typed atoms and untyped atoms. The retrospective ligand set with 4996 ligands were applied to test the model. ROC curves with AUC values were used for the performance calculation. Compounds were classified as active above a Shape similarity score of 0.56 (based on the minimum Euclidean distance from the [0;1] point, which represents ideal classification in the ROC plot with an AUC value of 1). The typed atom version of the volume scoring gave us the best model (AUC = 0.750) in the case of the retrospective set, its ROC plot is shown in Figure S3.

Pharmacophore screening. The pharmacophore modeling was carried out in Schrödinger, with the Phase package.[49] Actives below 100 nM and inactives above 10000 nM IC_{50} values were

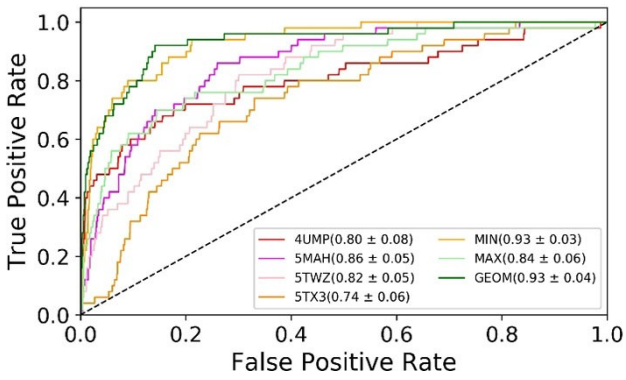

Figure 3. ROC curves with AUC values (and 95% confidence intervals[47]) of the retrospective docking. Ensemble docking based on the minimum, maximum and geometric mean of the seven docking scores is better than using any single structure. Based on our earlier results, we have selected the geometric mean from the available data fusion rules.[26]

selected for modeling from the ChEMBL data. The dataset was split into training and test sets. The training set contained 40 actives out of 50 ligands (with tautomers and stereoisomers), while the test set contained 10 actives out of 17 ligands in total. Altogether 50 actives (same as for docking and shape screening, see above) and 17 true inactives were thus used for training and validating the pharmacophore model. Moreover, the retrospective set for ligand docking was used as an additional test set. The best model is shown in Figure S3 (along with its ROC plot) and contains an H-bond acceptor, a hydrophobic group and two aromatic rings as pharmacophore features. It could retrieve 46 unique molecules out of the 50 actives, with an AUC value of 0.87. To be considered as a match, a ligand needed to fit at least 3 out of the 4 features. Compounds were classified as active above a Phase score of 1.857 (based on the minimum Euclidean distance from the [0;1] point, which represents ideal classification in the ROC plot with an AUC value of 1).

Data fusion. The final models (docking, pharmacophore and shape screening) were used for the in-house database screen. The results were used together to select the most prominent molecules for *in vitro* testing. A predicted active molecule was selected for the enzyme activity test, if at least two different models predicted it as active. Finally, 64 different molecules were selected for biochemical testing.

In vitro testing

MELK inhibition was evaluated according to the Z'-LYTE kinase inhibition assay format (Life Technologies). The assay is based on the different sensitivity of phosphorylated and non-phosphorylated peptides to proteolytic cleavage and applies a FRET-based readout. After incubating the kinase + substrate peptide (labeled) + test compound mixture for an hour, a development reaction is carried out, where any peptide that was not phosphorylated by the kinase is cleaved, disrupting the resonance energy transfer between the FRET pair (located on opposite ends of the substrate peptide). The reaction progress is quantified based on the ratio of the detected emission at 445 nm (coumarin) and 520 nm (fluorescein), i.e. the ratio of cleaved vs intact peptide. Interference with the development reaction and intrinsic fluorescence is tested for each datapoint as part of the assay protocol. A more detailed description of the assay is available on the website of Life Technologies.[50] First, percent inhibition values were determined at 10 μM for the 64 compounds, then IC_{50} values were determined for the molecules with single-point inhibition values above 40% (nine compounds). In addition, all further members of the [1,2,4]triazolo[1,5-*b*] isoquinoline scaffold were submitted to IC_{50} determinations as well. For some compounds, 50% inhibition was not reached within their window of solubility or assay interference was detected at high-concentration datapoints. In these cases, percent inhibition values at 10 μM are included in Table 1.

General procedures for reaction of 2,3-diamino-4-methylisoquinolinium 4-methylbenzenesulfonate with aryl aldehydes

To the solution of the appropriate 2,3-diamino-isoquinolinium 4-methylbenzenesulfonate derivatives (1 mmol) and the appropriate aryl aldehyde (5 mmol) in abs. ethanol (15 mL) DBU (0.7 mL) was added and the reaction mixture was stirred at room temperature for 24 hours. The deposited yellow crystals were filtered off and washed with ethanol. The product was recrystallized from ethanol (except ID-2126, ID-2128 which was recrystallized from EtOAc and ID-2133 which was recrystallized from DMF).

2-(3-chlorophenyl)-10-methyl-[1,2,4]triazolo[1,5-*b*] isoquinoline (3, ID-2125)

This compound was prepared from 2,3-diamino-4-methylisoquinolinium 4-methylbenzenesulfonate (345 mg, 1 mmol) and 3-chlorobenzaldehyde (567 μL, 703 mg, 5 mmol) to give the titled compound ID-2125 as yellow crystals (73 mg, 25%); mp. 199–202 °C; ^{1}H NMR (500 MHz, $CDCl_3$ + TFA): δ 9.51 (s, 1H), 8.26 (s, 1H), 8.22 (d, J = 9.63 Hz, 1H), 8.17 (d, J = 8.84 Hz, 2H), 7.95 (t, J = 7.75 Hz, 1H), 7.80 (t, J = 7.75 Hz, 1H), 7.58 (d, J = 9.21 Hz, 1H), 7.52 (t, J = 8.37 Hz, 1H), 3.08 (s, 3H); ^{13}C NMR (125 MHz, $CDCl_3$ + TFA): δ 157.0, 139.5, 135.5, 133.6, 133.3, 130.9, 129.2, 128.2, 127.8, 126.4, 124.8, 124.5, 123.3, 117.6, 116.2, 113.9, 12.6. HRMS (ESI): *m/z* calcd for $C_{17}H_{13}N_3Cl^+$: 294.0798 $[M+H]^+$; found: 294.0791

2-(4-methoxyphenyl)-10-methyl-[1,2,4]triazolo[1,5-*b*] isoquinoline (4, ID-2126)

This compound was prepared from 2,3-diamino-4-methylisoquinolinium 4-methylbenzenesulfonate (345 mg, 1 mmol) and 4-methoxybenzaldehyde (606 μL, 681 mg, 5 mmol) to give the titled compound ID-2126 as yellow crystals (9 mg, 31%); mp. 223–224 °C; ^{1}H NMR (500 MHz, $CDCl_3$ + TFA): δ 9.40 (s, 1H), 8.25 (d, J = 9.03 Hz, 2H), 8.15 (d, J = 8.36 Hz, 1H), 8.09 (d, J = 9.36 Hz, 1H), 7.86 (t, J = 8.02 Hz, 1H), 7.71 (t, J = 8.36 Hz, 1H), 7.00 (d, J = 9.03 Hz, 2H), 3.85 (s, 3H), 3.09 (s, 3H); ^{13}C NMR (125 MHz, $CDCl_3$ + TFA): δ 163.9, 157.9, 139.5, 135.0, 132.3, 130.2, 128.7, 128.5, 127.6, 124.2, 123.2, 117.0, 116.5, 114.9, 114.3, 114.0, 55.8, 12.6. HRMS (ESI): *m/z* calcd for $C_{18}H_{16}N_3O^+$: 290.1293 $[M+H]^+$; found: 290.1286

2-(3-methoxyphenyl)-10-methyl-[1,2,4]triazolo[1,5-*b*] isoquinoline (5, ID-2127)

This compound was prepared from 2,3-diamino-4-methylisoquinolinium 4-methylbenzenesulfonate (345 mg, 1 mmol) and 3-methoxybenzaldehyde (609 μL, 681 mg, 5 mmol) to give the titled compound ID-2127 as yellow crystals (82 mg, 28%); mp. 182–183 °C; ^{1}H NMR (500 MHz, $CDCl_3$): δ 9.20 (s, 1H), 8.00 (d, J = 7.39 Hz, 1H), 7.95 (s, 2H), 7.77 (d, J = 9.77 Hz, 1H), 7.48-7.40 (m, 2H), 7.35 (t, J = 7.39 Hz, 1H), 7.03 (d, J = 8.98 Hz, 1H), 3.94 (s, 3H), 3.05 (s, 3H); ^{13}C NMR (125 MHz, $CDCl_3$): δ 165.4, 159.9, 150.4, 132.5, 131.0, 129.6, 127.7, 126.5, 125.3, 123.8, 123.3, 122.4, 120.2, 119.3, 112.2, 55.4, 12.9. HRMS (ESI): *m/z* calcd for $C_{18}H_{16}N_3O^+$: 290.1293 $[M+H]^+$; found: 290.1290

2-(benzo[*d*][1,3]dioxol-5-yl)-10-methyl-[1,2,4]triazolo[1,5-*b*] isoquinoline (6, ID-2128)

This compound was prepared from 2,3-diamino-4-methylisoquinolinium 4-methylbenzenesulfonate (345 mg, 1 mmol) and piperonal (751 mg, 5 mmol) to give the titled compound ID-2128 as yellow crystals (95 mg, 31%); mp. 273–274 °C; ^{1}H NMR (500 MHz, $CDCl_3$ + TFA): δ 9.51 (s, 1H), 8.25 (d, J = 8.7 Hz, 1H), 8.16 (d, J = 8.7 Hz, 1H), 7.99 (t, J = 8.7 Hz, 1H), 7.83 (t, J = 7.76 Hz, 1H), 7.75 (d, J = 8.7 Hz, 1H), 7.63 (s, 1H), 7.02 (d, J = 9.62 Hz, 1H), 6.12 (s, 2H), 3.02 (s, 3H); ^{13}C NMR (125 MHz, $CDCl_3$ + TFA): δ 153.0, 149.1, 135.7, 133.7, 129.4, 128.3, 127.9, 124.2, 123.4, 117.7, 115.4, 113.2, 110.9, 109.5, 107.6, 102.5, 12.4. HRMS (ESI): *m/z* calcd for $C_{18}H_{14}N_3O_2^+$: 304.1086 $[M+H]^+$; found: 304.1085

10-methyl-2-(3-(trifluoromethyl)phenyl)-[1,2,4]triazolo[1,5-*b*] isoquinoline (7, ID-2130)

This compound was prepared from 2,3-diamino-4-methylisoquinolinium 4-methylbenzenesulfonate (345 mg, 1 mmol) and 3-(trifluoromethyl)benzaldehyde (669 μL, 870 mg, 5 mmol) to give the titled compound ID-2130 as yellow crystals (80 mg, 24%); mp. 202–203 °C; ^{1}H NMR (500 MHz, $CDCl_3$ + TFA): δ 9.52 (s, 1H), 8.60 (s, 1H), 8.54 (d, J = 7.47 Hz, 1H), 8.22 (d, J = 8.27 Hz, 1H), 8.16 (d, J = 9.08 Hz, 1H), 7.95–7.89 (m, 2H), 7.80–7.75 (m, 2H), 3.07 (s, 3H); ^{13}C NMR (125 MHz, $CDCl_3$ + TFA): δ 157.3, 140.1, 135.4, 133.1, 132.6(q), 132.3(q), 132.0(q), 131.8(q), 131.6, 130.3, 129.9, 129.1, 127.9, 127.7, 125.4, 124.5, 123.4, 118.0, 116.4, 114.1, 12.7. HRMS (ESI): *m/z* calcd for $C_{18}H_{13}N_3F_3^+$: 328.1061 $[M+H]^+$; found: 328.1056

10-methyl-2-(4-(trifluoromethyl)phenyl)-[1,2,4]triazolo[1,5-*b*] isoquinoline (8, ID-2131)

This compound was prepared from 2,3-diamino-4-methylisoquinolinium 4-methylbenzenesulfonate (345 mg, 1 mmol) and 4-(trifluoromethyl)benzaldehyde (668 μL, 871 mg, 5 mmol) to give the titled compound ID-2131 as yellow crystals (92 mg, 28%); mp. 182–183 °C; ^{1}H NMR (500 MHz, $CDCl_3$): δ 9.16 (s, 1H), 8.46 (d, J = 8.52 Hz, 2H), 7.92 (d, J = 9.78 Hz, 1H), 7.77–7.72 (m, 3H), 7.47 (t, J = 6.62 Hz, 1H), 7.36 (t, J = 6.62 Hz, 1H), 3.02 (s, 3H); ^{13}C NMR (125 MHz, $CDCl_3$): δ 163.8, 150.3, 134.5, 131.9, 131.6, 131.2, 128.0, 127.9, 126.5, 125.6, 125.5(q), 125.1, 123.9, 123.3, 123.0, 122.6, 119.7, 12.1. HRMS (ESI): *m/z* calcd for $C_{18}H_{13}N_3F_3^+$: 328.1061 $[M+H]^+$; found: 328.1056

10-methyl-2-(pyridin-3-yl)-[1,2,4]triazolo[1,5-*b*]isoquinoline (9, ID-2132)

This compound was prepared from 2,3-diamino-4-methylisoquinolinium 4-methylbenzenesulfonate (345 mg, 1 mmol) and pyridine-3-carboxaldehyde (472 μL, 535 mg, 5 mmol) to give the titled compound ID-2132 as yellow crystals (81 mg, 31%); mp. 234–238 °C; ^{1}H NMR (500 MHz, $CDCl_3$ + TFA): δ 9.77 (s, 1H), 9.38 (s, 1H), 9.34 (d, J = 7.77 Hz, 1H), 9.02 (d, J = 5.18 Hz, 2H), 8.13 (t, J = 6.22 Hz, 1H), 8.09 (d, J = 7.77 Hz, 1H), 7.96 (d, J = 8.29 Hz, 1H), 7.69 (t, J = 8.29 Hz, 1H), 7.58 (t, J = 8.03 Hz, 1H), 3.06 (s, 3H); ^{13}C NMR (125 MHz, $CDCl_3$ + TFA): δ 157.3, 147.4, 143.7, 143.1, 141.4, 133.1, 130.4, 127.4, 127.0, 125.8, 123.8, 120.3, 116.3, 114.0, 12.8. HRMS (ESI): *m/z* calcd for $C_{16}H_{13}N_4^+$: 261.1140 $[M+H]^+$; found: 261.1136

2-(6-chloropyridin-3-yl)-10-methyl-[1,2,4]triazolo[1,5-*b*] isoquinoline (10, ID-2133)

This compound was prepared from 2,3-diamino-4-methylisoquinolinium 4-methylbenzenesulfonate (345 mg, 1 mmol) and 6-chloropyridine-3-carboxaldehyde (708 mg, 5 mmol) to give the titled compound ID-2133 as yellow crystals (75 mg, 25%); mp. 289–290 °C; ^{1}H NMR (500 MHz, $CDCl_3$ + TFA): δ 9.59 (s, 1H), 9.40 (s, 1H), 8.73 (d, J = 8.74 Hz, 1H), 8.27 (d, J = 9.51 Hz, 1H), 8.02 (t, J = 6.42 Hz, 1H), 7.86 (t, J = 7.20 Hz, 1H), 7.75 (d, J = 8.74 Hz, 1H), 3.07 (s, 3H); ^{13}C NMR (125 MHz, $CDCl_3$ + TFA): δ 155.4, 148.1, 139.7, 136.0, 134.0, 129.7, 128.8, 128.0, 126.3, 124.8, 123.3, 119.9, 118.1, 115.8, 113.6, 111.1, 12.5. HRMS (ESI): *m/z* calcd for $C_{16}H_{12}N_4Cl^+$: 295.075 $[M+H]^+$; found: 295.0745

10-methyl-2-(pyridin-2-yl)-[1,2,4]triazolo[1,5-*b*]isoquinoline (11, ID-2134)

This compound was prepared from 2,3-diamino-4-methylisoquinolinium 4-methylbenzenesulfonate (345 mg, 1 mmol) and pyridine-2-carboxaldehyde (478 μL, 535 mg, 5 mmol) to give the titled compound ID-2134 as yellow crystals (75 mg, 29%); mp. 238–240 °C; ^{1}H NMR (500 MHz, $CDCl_3$): δ 9.31 (s, 1H), 8.86 (s, 1H), 8.47 (d, J = 6.75 Hz, 1H), 8.02 (d, J = 9.00 Hz, 1H), 7.89–7.84 (m, 2H), 7.52 (t, J = 8.04 Hz, 1H), 7.42–7.39 (m, 2H), 3.12 (s, 3H); ^{13}C NMR (125 MHz, $CDCl_3$): δ 164.7, 150.6, 150.2, 150.1, 136.7, 131.3, 128.0, 126.6, 125.6, 124.5, 124.3, 123.4, 123.1, 122.8, 120.3, 13.1. HRMS (ESI): *m/z* calcd for $C_{16}H_{13}N_4^+$: 261.1140 $[M+H]^+$; found: 261.1139. *m/z* calcd for $C_{16}H_{12}N_4Na^+$: 283.0959 $[M+Na]^+$; found: 283.0960

10-methyl-2-(pyridin-4-yl)-[1,2,4]triazolo[1,5-*b*]isoquinoline (12, ID-2135)

This compound was prepared from 2,3-diamino-4-methylisoquinolinium 4-methylbenzenesulfonate (345 mg, 1 mmol) and pyridine-4-carboxaldehyde (473 μL, 535 mg, 5 mmol) to give the titled compound ID-2135 as yellow crystals (54 mg, 21%); mp. 230–232 °C; ^{1}H NMR (500 MHz, $CDCl_3$ + TFA): δ 9.64 (s, 1H), 9.23 (d, J = 7.72 Hz, 2H), 8.86 (d, J = 6.90 Hz, 2H), 8.29 (d, J = 8.55 Hz, 1H), 8.22 (d, J = 8.55 Hz, 1H), 8.02 (t, J = 6.90 Hz, 1H), 7.86 (t, J = 7.72 Hz, 1H), 3.13 (s, 3H); ^{13}C NMR (125 MHz, $CDCl_3$ + TFA): δ 154.2, 143.2, 136.3, 132.9, 130.1, 128.3, 127.8, 125.9, 125.0, 123.6, 119.5, 117.9, 115.6, 113.3, 111.1, 12.8. HRMS (ESI): *m/z* calcd for $C_{16}H_{13}N_4^+$: 261.1140 $[M+H]^+$; found: 261.1137

2-(2,4-dichlorophenyl)-10-methyl-[1,2,4]triazolo[1,5-*b*] isoquinoline (13, ID-2136)

This compound was prepared from 2,3-diamino-4-methylisoquinolinium 4-methylbenzenesulfonate (345 mg, 1 mmol) and 2,4-dichlorobenzaldehyde (875 mg, 5 mmol) to give the titled compound ID-2136 as yellow crystals (105 mg, 32%); mp. 190–192 °C; ^{1}H NMR (500 MHz, $CDCl_3$ + TFA): δ 9.49 (s, 1H), 8.18 (d, J = 9.51 Hz, 1H), 8.08 (d, J = 7.96 Hz, 1H), 7.92 (d, J = 8.74 Hz, 1H), 7.86 (t, J = 6.17 Hz, 1H), 7.71 (t, J = 7.84 Hz, 1H), 7.59 (s, 1H), 7.45 (d, J = 8.35 Hz, 1H), 3.09 (s, 3H); ^{13}C NMR (125 MHz, $CDCl_3$ + TFA): δ 157.6, 141.7, 138.9, 134.6, 133.1, 132.1, 130.9, 128.3, 127.8, 127.4, 127.1, 124.0, 123.3, 118.5, 116.5, 114.2, 12.8. HRMS (ESI): *m/z* calcd for $C_{17}H_{12}N_3Cl_2^+$: 328.0408 $[M+H]^+$; found: 328.0409

2-(3,4-dichlorophenyl)-10-methyl-[1,2,4]triazolo[1,5-*b*] isoquinoline (14, ID-2137)

This compound was prepared from 2,3-diamino-4-methylisoquinolinium 4-methylbenzenesulfonate (345 mg, 1 mmol) and 3,4-dichlorobenzaldehyde (875 mg, 5 mmol) to give the titled compound ID-2137 as yellow crystals (80 mg, 24%); mp. 236–238 °C; ^{1}H NMR (500 MHz, $CDCl_3$ + TFA): δ 9.56 (s, 1H), 8.35 (s, 1H), 8.25 (d, J = 23.61 Hz, 2H), 8.06 (d, J = 22.68 Hz, 2H), 7.88 (s, 1H), 7.72 (s, 1H), 3.06 (s, 3H); ^{13}C NMR (125 MHz, $CDCl_3$ + TFA): δ 155.8, 139.1, 136.0, 134.0, 131.9, 129.9, 128.7, 128.0, 127.0, 124.8, 123.3, 117.4, 115.7, 113.4, 111.1, 12.5. HRMS (ESI): *m/z* calcd for $C_{17}H_{12}N_3Cl_2^+$: 328.0408 $[M+H]^+$; found: 328.0409

2-(2-chlorophenyl)-10-ethyl-[1,2,4]triazolo[1,5-*b*]isoquinoline (15, ID-2138)

This compound was prepared from 2,3-diamino-4-ethylisoquinolinium 4-methylbenzenesulfonate (359 mg, 1 mmol) and 2-chlorobenzaldehyde (563 μL, 703 mg, 5 mmol) to give the titled compound ID-2138 as yellow crystals (80 mg, 26%); mp. 157–158 °C; ^{1}H NMR (500 MHz, $CDCl_3$ + TFA): δ 9.58 (s, 1H), 8.28 (d, J = 9.41 Hz, 1H), 8.19 (d, J = 8.20 Hz, 1H), 7.97 (t, J = 6.68 Hz, 1H), 7.92 (d, J = 8.50 Hz, 1H), 7.81 (t, J = 7.59 Hz, 1H), 7.63–7.58 (m, 2H), 7.51 (t, J = 6.68 Hz,

1H), 3.58 (q, J_1 = 6.73 Hz, J_2 = 7.18 Hz, 2H), 1.46 (t, J = 8.07 Hz, 3H); ^{13}C NMR (125 MHz, $CDCl_3$ + TFA): δ 156.1, 138.5, 134.9, 133.9, 133.4, 132.2, 131.1, 129.1, 128.3, 128.0, 127.6, 124.8, 123.8, 123.1, 116.2, 113.9, 21.1, 14.3. HRMS (ESI): *m/z* calcd for $C_{18}H_{15}N_3Cl^+$: 308.0954 [M + H]$^+$; found: 308.0951

2-(3-chlorophenyl)-10-ethyl-[1,2,4]triazolo[1,5-*b*]isoquinoline (16, ID-2139)

This compound was prepared from 2,3-diamino-4-ethylisoquinolinium 4-methylbenzenesulfonate (359 mg, 1 mmol) and 3-chlorobenzaldehyde (567 μL, 703 mg, 5 mmol) to give the titled compound ID-2139 as yellow crystals (94 mg, 30%); mp. 186–187 °C; ^{1}H NMR (500 MHz, $CDCl_3$ + TFA): δ 9.49 (s, 1H), 8.27 (s, 1H), 8.22 (t, J = 7.75 Hz, 2H), 8.15 (d, J = 7.76 Hz, 1H), 7.93 (t, J = 7.75 Hz, 1H), 7.77 (t, J = 7.12 Hz, 1H), 7.56 (d, J = 8.37 Hz, 1H), 7.51 (t, J = 7.75 Hz, 1H), 3.58 (q, J_1 = 7.24 Hz, J_2 = 7.71 Hz, 2H), 1.46 (t, J = 9.16 Hz, 3H); ^{13}C NMR (125 MHz, $CDCl_3$ + TFA): δ 157.3, 139.5, 135.8, 134.6, 133.4, 130.8, 128.9, 128.2, 127.9, 126.6, 125.1, 124.7, 123.9, 123.0, 116.5, 114.2, 111.9, 20.6, 14.0. HRMS (ESI): *m/z* calcd for $C_{18}H_{15}N_3Cl^+$: 308.0954 [M + H]$^+$; found: 308.0953

2-(4-chlorophenyl)-10-ethyl-[1,2,4]triazolo[1,5-*b*]isoquinoline (17, ID-2140)

This compound was prepared from 2,3-diamino-4-ethylisoquinolinium 4-methylbenzenesulfonate (359 mg, 1 mmol) and 4-chlorobenzaldehyde (703 mg, 5 mmol) to give the titled compound ID-2140 as yellow crystals (136 mg, 44%); mp. 197–199 °C; ^{1}H NMR (500 MHz, $CDCl_3$ + TFA): δ 9.52 (s, 1H), 8.26 (d, J = 8.95 Hz, 1H), 8.21–8.18 (m, 3H), 7.98 (t, J = 6.77 Hz, 1H), 7.82 (t, J = 8.73 Hz, 1H), 7.56 (d, J = 8.30 Hz, 1H), 3.53 (q, J_1 = 8.04 Hz, J_2 = 7.55 Hz, 2H), 1.45 (t, J = 7.54 Hz, 3H); ^{13}C NMR (125 MHz, $CDCl_3$ + TFA): δ 157.5, 141.7, 138.5, 135.6, 133.2, 130.0, 129.5, 128.4, 128.1, 124.9, 123.0, 121.3, 118.3, 116.0, 113.7, 111.4, 20.5, 13.7. HRMS (ESI): *m/z* calcd for $C_{18}H_{15}N_3Cl^+$: 308.0954 [M + H]$^+$; found: 308.0957

10-ethyl-2-(4-methoxyphenyl)-[1,2,4]triazolo[1,5-*b*] isoquinoline (18, ID-2141)

This compound was prepared from 2,3-diamino-4-ethylisoquinolinium 4-methylbenzenesulfonate (359 mg, 1 mmol) and 4-methoxybenzaldehyde (606 μL, 681 mg, 5 mmol) to give the titled compound ID-2141 as yellow crystals (140 mg, 46%); mp. 193–195 °C; ^{1}H NMR (500 MHz, $CDCl_3$ + TFA): δ 9.44 (s, 1H), 8.26 (d, J = 9.23 Hz, 1H), 8.14 (d, J = 9.23 Hz, 3H), 7.94 (t, J = 8.34 Hz, 1H), 7.77 (t, J = 6.55 Hz, 1H), 6.98 (d, J = 8.44 Hz, 2H), 3.80 (s, 3H), 3.50 (q, J_1 = 7.47 Hz, J_2 = 8.09 Hz, 2H), 1.44 (t, J = 7.46 Hz, 3H); ^{13}C NMR (125 MHz, $CDCl_3$ + TFA): δ 164.9, 156.4, 139.1, 134.5, 133.2, 130.1, 128.9, 128.6, 128.0, 124.7, 122.9, 122.6, 116.2, 114.9, 114.7, 113.9, 111.6, 55.4, 20.0, 15.4. HRMS (ESI): *m/z* calcd for $C_{19}H_{18}N_3O^+$: 304.1449 [M + H]$^+$; found: 304.1446

10-ethyl-2-(3-methoxyphenyl)-[1,2,4]triazolo[1,5-*b*] isoquinoline (19, ID-2142)

This compound was prepared from 2,3-diamino-4-ethylisoquinolinium 4-methylbenzenesulfonate (359 mg, 1 mmol) and 3-methoxybenzaldehyde (609 μL, 681 mg, 5 mmol) to give the titled compound ID-2142 as yellow crystals (75 mg, 23%); mp. 182–183 °C; ^{1}H NMR (500 MHz, $CDCl_3$ + TFA): δ 9.44 (s, 1H), 8.19 (d, J = 8.70 Hz, 1H), 8.11 (d, J = 9.03 Hz, 1H), 7.90–7.83 (m, 2H), 7.78 (s, 1H), 7.72 (t, J = 8.06 Hz, 1H), 7.38 (t, J = 7.10 Hz, 1H), 7.05 (d, J = 9.99 Hz, 1H), 3.85 (s, 3H), 3.56 (q, J_1 = 8.30 Hz, J_2 = 7.79 Hz, 2H), 1.45 (t, J = 8.30 Hz, 3H); ^{13}C NMR (125 MHz, $CDCl_3$ + TFA): δ 159.0, 139.6, 134.3, 132.7, 130.4, 128.6, 127.8, 124.6, 123.6, 123.0, 120.7, 120.5, 116.7, 114.4, 112.2, 55.4, 20.6, 14.0. HRMS (ESI): *m/z* calcd for $C_{19}H_{18}N_3O^+$: 304.1449 [M + H]$^+$; found: 304.1456

2-(3-chlorophenyl)-[1,2,4]triazolo[1,5-*b*]isoquinoline (20, ID-2145)

To the solution of 2,3-diamino-isoquinolinium 4-methylbenzenesulfonate (0.662 g, 2 mmol) and 3-chlorobenzaldehyde (1135 μL, 1.4 g, 10 mmol) in abs acetonitrile (30 mL) was added molecular sieves (5.0 g, FLUKA, UOP type, 4 A°) and the mixture was boiled at 82 °C for 48 hours. The reaction mixture was filtered and evaporated. The residue was chromatographed over Al_2O_3 neutral by using hexane:EtOAc 4:1 as eluent. Yellow crystals (100 mg, 36%); mp. 296–297 °C; ^{1}H NMR (500 MHz, $CDCl_3$ + TFA): δ 9.66 (s, 1H), 8.57 (s, 1H), 8.22 (d, J = 19.50 Hz, 3H), 7.96 (t, J = 64.82 Hz, 3H), 7.62 (d, J = 40.58 Hz, 2H); ^{13}C NMR (125 MHz, $CDCl_3$ + TFA): δ 156.5, 139.5, 137.4, 136.1, 134.2, 131.1, 130.6, 129.9, 128.1, 127.1, 126.1, 124.3, 115.8, 113.5, 107.7. HRMS (ESI): *m/z* calcd for $C_{16}H_{11}N_3Cl^+$: 280.0641 [M + H]$^+$; found: 280.0640

2-(3-tolyl)-[1,2,4]triazolo[1,5-*b*]isoquinoline (21, ID-2147)

To the solution of 2,3-diamino-isoquinolinium 4-methylbenzenesulfonate (0.662 g, 2 mmol) and 3-methylbenzaldehyde (1175 μL, 1.2 g, 10 mmol) in abs acetonitrile (30 mL) was added molecular sieves (4.0 g, FLUKA, UOP type, 4 A°) and the mixture was boiled at 82 °C for 48 hours. The reaction mixture was filtered and evaporated. The residue was chromatographed over Al_2O_3 neutral by using hexane:EtOAc 4:1 as eluent. Yellow crystals (96 mg, 37%); mp. 271–272 °C; ^{1}H NMR (500 MHz, $CDCl_3$ + TFA): δ 9.60 (s, 1H), 8.56 (s, 1H), 8.15 (t, J = 7.92 Hz, 2H), 8.00 (s, 2H), 7.91 (t, J = 7.71 Hz, 1H), 7.78 (t, J = 7.71 Hz, 1H), 7.47 (s, 2H), 2.46 (s, 3H); ^{13}C NMR (125 MHz, $CDCl_3$ + TFA): δ 158.1, 140.0, 137.1, 134.9, 133.7, 130.3, 129.5, 128.4, 127.0, 125.2, 124.4, 122.5, 116.2, 113.9, 107.5, 21.0. HRMS (ESI): *m/z* calcd for $C_{17}H_{14}N_3^+$: 260.1187 [M + H]$^+$; found: 260.1185

This article belongs to the Early-Career Special Collection, "EuroMedChem Talents".

Acknowledgements

The authors thank their colleagues at the MS Metabolomics Laboratory Core Facility at RCNS for the HRMS measurements, and Károly Héberger for helpful discussions. The work of A.R. is supported by the National Research, Development and Innovation Office of Hungary (OTKA, contract no. PD134416). The work of D.B. is supported by the János Bolyai Research Scholarship of the Hungarian Academy of Sciences and the ÚNKP-21-5 New National Excellence Program of the Ministry for Innovation and Technology.

Conflict of Interest

The authors declare that they have no conflict of interest.

Keywords: MELK inhibitor · virtual screening · kinase · docking · isoquinoline

[1] B. S. Heyer, J. Warsowe, D. Solter, B. B. Knowles, S. L. Ackerman, *Mol. Reprod. Dev.* **1997**, *47*, 148–156.
[2] P. Jiang, D. Zhang, *Int. J. Mol. Sci. 2013, Vol. 14, Pages 21551–21560* **2013**, *14*, 21551–21560.
[3] Q. Tang, W. Li, X. Zheng, L. Ren, J. Liu, S. Li, J. Wang, G. Du, *Signal Transduct. Target. Ther. 2020 51* **2020**, *5*, 1–12.
[4] D. Gray, A. M. Jubb, D. Hogue, P. Dowd, N. Kljavin, S. Yi, W. Bai, G. Frantz, Z. Zhang, H. Koeppen, F. J. de Sauvage, D. P. Davis, *Cancer Res.* **2005**, *65*, 9751–9761.
[5] S. Choi, J. L. Ku, *Biochem. Biophys. Res. Commun.* **2011**, *412*, 207–213.
[6] R. Kuner, M. Fälth, N. C. Pressinotti, J. C. Brase, S. B. Puig, J. Metzger, S. Gade, G. Schäfer, G. Bartsch, E. Steiner, H. Klocker, H. Sültmann, *J. Mol. Med. 2012 912* **2012**, *91*, 237–248.
[7] B. Ryu, D. S. Kim, A. M. DeLuca, R. M. Alani, *PLoS One* **2007**, *2*, e594.
[8] R. Janostiak, N. Rauniyar, T. T. Lam, J. Ou, L. J. Zhu, M. R. Green, N. Wajapeyee, *Cell Rep.* **2017**, *21*, 2829–2841.
[9] S. Chung, H. Suzuki, T. Miyamoto, N. Takamatsu, A. Tatsuguchi, K. Ueda, K. Kijima, Y. Nakamura, Y. Matsuo, *Oncotarget* **2012**, *3*, 1629–1640.
[10] W. Ji, C. Arnst, A. R. Tipton, M. E. B. II, W. R. Taylor, T. J. Yen, S.-T. Liu, *PLoS One* **2016**, *11*, e0153518.
[11] M. H. Meel, M. C. de Gooijer, M. G. Navarro, P. Waranecki, M. Breur, L. C. M. Buil, L. E. Wedekind, J. W. R. Twisk, J. Koster, R. Hashizume, E. H. Raabe, A. M. Carcaboso, M. Bugiani, O. van Tellingen, D. G. van Vuurden, G. J. L. Kaspers, E. Hulleman, *Clin. Cancer Res.* **2018**, *24*, 5645–5657.
[12] H. Alachkar, M. B. G. Mutonga, K. H. Metzeler, N. Fulton, G. Malnassy, T. Herold, K. Spiekermann, S. K. Bohlander, W. Hiddemann, Y. Matsuo, W. Stock, Y. Nakamura, *Oncotarget* **2014**, *5*, 12371–12382.
[13] L. Beke, C. Kig, J. T. M. Linders, S. Boens, A. Boeckx, E. van Heerde, M. Parade, A. De Bondt, I. Van den Wyngaert, T. Bashir, S. Ogata, L. Meerpoel, A. Van Eynde, C. N. Johnson, M. Beullens, D. Brehmer, M. Bollen, *Biosci. Rep.* **2015**, *35*, 267.
[14] R. Edupuganti, J. M. Taliaferro, Q. Wang, X. Xie, E. J. Cho, F. Vidhu, P. Ren, E. V. Anslyn, C. Bartholomeusz, K. N. Dalby, *Bioorg. Med. Chem.* **2017**, *25*, 2609–2616.
[15] M. Harger, J.-H. Lee, B. Walker, J. M. Taliaferro, R. Edupuganti, K. N. Dalby, P. Ren, *J. Mol. Model.* **2019**, *25*, 151.
[16] E. Jaune, E. Cavazza, C. Ronco, O. Grytsai, P. Abbe, N. Tekaya, M. Zerhouni, G. Beranger, L. Kaminski, F. Bost, M. Gesson, M. Tulic, P. Hofman, R. Ballotti, T. Passeron, T. Botton, R. Benhida, S. Rocchi, *Cell Death Dis.* **2021**, *12*, 64.
[17] R. Wang, Y. Chen, B. Yang, S. Yu, X. Zhao, C. Zhang, C. Hao, D. Zhao, M. Cheng, *Bioorg. Chem.* **2020**, *94*, 103474.
[18] K. V. Mahasenan, C. Li, *J. Chem. Inf. Model.* **2012**, *52*, 1345–55.
[19] H. M. Berman, J. Westbrook, Z. Feng, G. Gilliland, T. N. Bhat, H. Weissig, I. N. Shindyalov, P. E. Bourne, *Nucleic Acids Res.* **2000**, *28*, 235–42.
[20] "RCSB Protein Data Bank," can be found under https://www.rcsb.org/ (Accessed 29 Sep 2021), **2021**.
[21] M. Rachman, D. Bajusz, A. Hetényi, A. Scarpino, B. Merő, A. Egyed, L. Buday, X. Barril, G. M. Keserű, *RSC Med. Chem.* **2020**, *11*, 552–558.
[22] L. Petri, A. Egyed, D. Bajusz, T. Imre, A. Hetényi, T. Martinek, P. Ábrányi-Balogh, G. M. Keserű, *Eur. J. Med. Chem.* **2020**, *207*, 112836.
[23] A. Gaulton, L. J. Bellis, A. P. Bento, J. Chambers, M. Davies, A. Hersey, Y. Light, S. McGlinchey, D. Michalovich, B. Al-Lazikani, J. P. Overington, *Nucleic Acids Res.* **2012**, *40*, D1100–7.
[24] "ChEMBL database (release 29)," can be found under https://www.ebi.ac.uk/chembl/ (Accessed 28 Sep 2021), **2021**.
[25] M. M. Mysinger, M. Carchia, J. J. Irwin, B. K. Shoichet, *J. Med. Chem.* **2012**, *55*, 6582–6594.
[26] D. Bajusz, A. Rácz, K. Héberger, *Molecules* **2019**, *24*, 2690.
[27] G. W. Bemis, M. A. Murcko, *J. Med. Chem.* **1996**, *39*, 2887–2893.
[28] A. Egyed, D. Bajusz, G. M. Keserű, *Bioorg. Med. Chem.* **2019**, *27*, 1497–1508.
[29] S. Ueda, H. Nagasawa, *J. Am. Chem. Soc.* **2009**, *131*, 15080–15081.
[30] L. Filák, Z. Riedl, O. Egyed, M. Czugler, C. N. Hoang, J. G. Schantl, G. Hajós, *Tetrahedron* **2008**, *64*, 1101–1113.
[31] K. P. Rembacz, K. M. Zrubek, P. Golik, K. Michalik, J. Bogusz, B. Wladyka, M. Romanowska, G. Dubin, *Arch. Biochem. Biophys.* **2019**, *671*, 1–7.
[32] B. B. Touré, J. Giraldes, T. Smith, E. R. Sprague, Y. Wang, S. Mathieu, Z. Chen, Y. Mishina, Y. Feng, Y. Yan-Neale, S. Shakya, D. Chen, M. Meyer, D. Puleo, J. T. Brazell, C. Straub, D. Sage, K. Wright, Y. Yuan, X. Chen, J. Duca, S. Kim, L. Tian, E. Martin, K. Hurov, W. Shao, *J. Med. Chem.* **2016**, *59*, 4711–4723.
[33] D. Bajusz, G. G. Ferenczy, G. M. Keserű, *Curr. Top. Med. Chem.* **2017**, *17*, 2235–2259.
[34] The Uniprot Consortium, *Nucleic Acids Res.* **2021**, *49*, D480–D489.
[35] "UniProt database," can be found under https://www.uniprot.org/ (Accessed 29 Sep 2021), **2021**.
[36] "RDKit: Open-Source Cheminformatics Software," can be found under http://rdkit.org/ (Accessed 29 Sep 2021), **2021**.
[37] M. R. Berthold, N. Cebron, F. Dill, T. R. Gabriel, T. Kötter, T. Meinl, P. Ohl, K. Thiel, B. Wiswedel, *SIGKDD Explor. Newsl.* **2009**, *11*, 26–31.
[38] G. M. Sastry, M. Adzhigirey, T. Day, R. Annabhimoju, W. Sherman, *J. Comput.-Aided Mol. Des.* **2013**, *27*, 221–34.
[39] P. Virtanen, R. Gommers, T. E. Oliphant, M. Haberland, T. Reddy, D. Cournapeau, E. Burovski, P. Peterson, W. Weckesser, J. Bright, S. J. van der Walt, M. Brett, J. Wilson, K. J. Millman, N. Mayorov, A. R. J. Nelson, E. Jones, R. Kern, E. Larson, C. J. Carey, İ. Polat, Y. Feng, E. W. Moore, J. VanderPlas, D. Laxalde, J. Perktold, R. Cimrman, I. Henriksen, E. A. Quintero, C. R. Harris, A. M. Archibald, A. H. Ribeiro, F. Pedregosa, P. van Mulbregt, A. Vijaykumar, A. Pietro Bardelli, A. Rothberg, A. Hilboll, A. Kloeckner, A. Scopatz, A. Lee, A. Rokem, C. N. Woods, C. Fulton, C. Masson, C. Häggström, C. Fitzgerald, D. A. Nicholson, D. R. Hagen, D. V. Pasechnik, E. Olivetti, E. Martin, E. Wieser, F. Silva, F. Lenders, F. Wilhelm, G. Young, G. A. Price, G. L. Ingold, G. E. Allen, G. R. Lee, H. Audren, I. Probst, J. P. Dietrich, J. Silterra, J. T. Webber, J. Slavič, J. Nothman, J. Buchner, J. Kulick, J. L. Schönberger, J. V. de Miranda Cardoso, J. Reimer, J. Harrington, J. L. C. Rodríguez, J. Nunez-Iglesias, J. Kuczynski, K. Tritz, M. Thoma, M. Newville, M. Kümmerer, M. Bolingbroke, M. Tartre, M. Pak, N. J. Smith, N. Nowaczyk, N. Shebanov, O. Pavlyk, P. A. Brodtkorb, P. Lee, R. T. McGibbon, R. Feldbauer, S. Lewis, S. Tygier, S. Sievert, S. Vigna, S. Peterson, S. More, T. Pudlik, T. Oshima, T. J. Pingel, T. P. Robitaille, T. Spura, T. R. Jones, T. Cera, T. Leslie, T. Zito, T. Krauss, U. Upadhyay, Y. O. Halchenko, Y. Vázquez-Baeza, *Nat. Methods* **2020**, *17*, 261–272.
[40] G. Canevari, S. R. Depaolini, U. Cucchi, J. A. Bertrand, E. Casale, C. Perrera, B. Forte, P. Carpinelli, E. R. Felder, *Biochemistry* **2013**, *52*, 6380–6387.
[41] C. N. Johnson, V. Berdini, L. Beke, P. Bonnet, D. Brehmer, J. E. Coyle, P. J. Day, M. Frederickson, E. J. E. Freyne, R. A. H. J. Gilissen, C. C. F. Hamlett, S. Howard, L. Meerpoel, R. McMenamin, S. Patel, D. C. Rees, A. Sharff, F. Sommen, T. Wu, J. T. M. Linders, *ACS Med. Chem. Lett.* **2014**, *6*, 25–30.
[42] S. Klaeger, S. Heinzlmeir, M. Wilhelm, H. Polzer, B. Vick, P. A. Koenig, M. Reinecke, B. Ruprecht, S. Petzoldt, C. Meng, J. Zecha, K. Reiter, H. Qiao, D. Helm, H. Koch, M. Schoof, G. Canevari, E. Casale, S. Re Depaolini, A. Feuchtinger, Z. Wu, T. Schmidt, L. Rueckert, W. Becker, J. Huenges, A. K. Garz, B. O. Gohlke, D. P. Zolg, G. Kayser, T. Vooder, R. Preissner, H. Hahne, N. Tõnisson, K. Kramer, K. Götze, F. Bassermann, J. Schlegl, H. C. Ehrlich, S. Aiche, A. Walch, P. A. Greif, S. Schneider, E. R. Felder, J. Ruland, G. Médard, I. Jeremias, K. Spiekermann, B. Kuster, *Science* **2017**, *358*, eaan4368.
[43] H. T. Huang, H. S. Seo, T. Zhang, Y. Wang, B. Jiang, Q. Li, D. L. Buckley, B. Nabet, J. M. Roberts, J. Paulk, S. Dastjerdi, G. E. Winter, H. McLauchlan, J. Moran, J. E. Bradner, M. J. Eck, S. Dhe-Paganon, J. J. Zhao, N. S. Gray, *eLife* **2017**, *6*, e26693.
[44] R. A. Friesner, J. L. Banks, R. B. Murphy, T. A. Halgren, J. J. Klicic, D. T. Mainz, M. P. Repasky, E. H. Knoll, M. Shelley, J. K. Perry, D. E. Shaw, P. Francis, P. S. Shenkin, *J. Med. Chem.* **2004**, *47*, 1739–1749.
[45] T. A. Halgren, R. B. Murphy, R. A. Friesner, H. S. Beard, L. L. Frye, W. T. Pollard, J. L. Banks, *J. Med. Chem.* **2004**, *47*, 1750–1759.
[46] A. Rácz, D. Bajusz, K. Héberger, *Molecules* **2019**, *24*, 2811.
[47] A. Nicholls, *J. Comput.-Aided Mol. Des.* **2014**, *28*, 887–918.
[48] G. M. Sastry, S. L. Dixon, W. Sherman, *J. Chem. Inf. Model.* **2011**, *51*, 2455–2466.
[49] S. L. Dixon, A. M. Smondyrev, S. N. Rao, *Chem. Biol. Drug Des.* **2006**, *67*, 370–372.
[50] "Z'-LYTE Biochemical Kinase Assays.," can be found under http://www.lifetechnologies.com/hu/en/home/life-science/drug-discovery/target-and-lead-identification-and-validation/kinasebiology/kinase-activity-assays/z-lyte.html (Accessed 5 Aug 2021), **2021**.

Manuscript received: August 24, 2021
Revised manuscript received: October 6, 2021
Accepted manuscript online: October 10, 2021
Version of record online: October 19, 2021